The following supplements accompany the article

Monitoring the gray whale sound exposure mitigation zone and estimating acoustic transmission during a 4-D seismic survey, Sakhalin Island, Russia

Roberto Racca*, Melanie Austin, Alexander Rutenko, Koen Bröker

*Corresponding author: roberto.racca@jasco.com

Endangered Species Research 29: 131–146 (2015)

Supplement 1. The information contained in this Supplement provides details of the equipment used to record and transmit the underwater acoustic signals.

Fig. S1a shows schematically the deployment configuration of a telemetric system, consisting of a pre-amplified hydrophone in an independent vibration-absorbing pyramidal mount located 15 m away from the nearest component, two pressure containers in titanium alloy rated to depths of 100 m, and a radio buoy at the sea surface. Fig. S1b shows a block diagram of the circuitry in the various modules. Container 1 houses the autonomous underwater acoustic recorder, a detailed description of which was given in Borisov *et al.* (2008). It also contains the encoder for the telemetry system, which outputs a data stream over an RS-485 link, and three sealed lead–gel batteries with a total electric capacity of 115 A/h which supply power for the acoustic recorder and encoder. Container 2 houses the batteries powering the radio transmitter in the surface buoy. Modules consisting of eight 7.5V alkaline lantern batteries in series supply a 60V initial voltage with a capacity of ≈47 A/h. The pressure case can house three of these modules connected in parallel through protective diodes, providing a power source with a 60V initial voltage and ≈140A/h capacity. Container 2 is connected to the surface buoy by a 100m length strengthened cable with conductors for power and the RS-485 data link. The buoy contains the data link interface, radio transmitter, and a DC/DC converter producing a stabilized 10V supply. Kovzel & Rutenko (2009) describe in detail the digital modulation approach implemented in the telemetry encoder; in brief the output from the analogue to digital conversion (a Non Return to Zero or NRZ serial code, in which the binary output is represented by two electrical states potentially sustained over long sequences of repeated 1's or 0's) is converted to an Offset Quadrature Phase-Shift Keying (OQPSK) sequence in which there can be at most two clock cycles with no state changes. This greatly simplifies the synchronization at the receiving end of the telemetry data channel and increases noise immunity. This encoding is much more suitable for transmission over a radio communication link than the initial NRZ code. The minimum radio channel bandwidth necessary for transmission of the encoded signal is 37.5 kHz; in practice a spectrum width of ±100 kHz relative to the carrier frequency was assumed for channel separation between the

various transmitters deployed for acoustic monitoring along the PML. The radio stations operated within a specially licensed VHF band, with emitted RF power between 0.5 and 5.0 W.

A modified commercial multiband radio scanner is used to receive the radio telemetry signal from each station. The signal from its audio output is applied to the decoder system, whose block diagram appears at the bottom of Fig. S1b. The decoder restores the clock signals from the OQPSK code and reconstructs the original binary NRZ sequence; it also detects bit failures in the received data words and compensates for them in such a way as to minimize resulting distortions of the digitized acoustic signal (Kovzel & Rutenko 2009). The decoded data streams from the nine acoustic monitoring stations along the PML were processed by a front-end notebook PC that performed diagnostic visualization functions in both time and frequency domains and packaged the data in one-minute files that were distributed over a local network to other notebook PCs for pulse level analysis and cross-comparison to model based estimations.

Literature Cited

Borisov SV, Kovzel DG, Rutenko AN, Ushchipovskii VG (2008) Stand-alone hydro acoustic station with radio channel for the acoustic measurements on the Shelf. Instrum Exp Tech 51:762

Kovzel DG, Rutenko AN (2009) A Self-Contained Acoustic Station with a Digital Radiotelemetry Channel for Monitoring Seismic Acoustic Signals on the Shelf. Instrum Exp Tech 52:857

a)

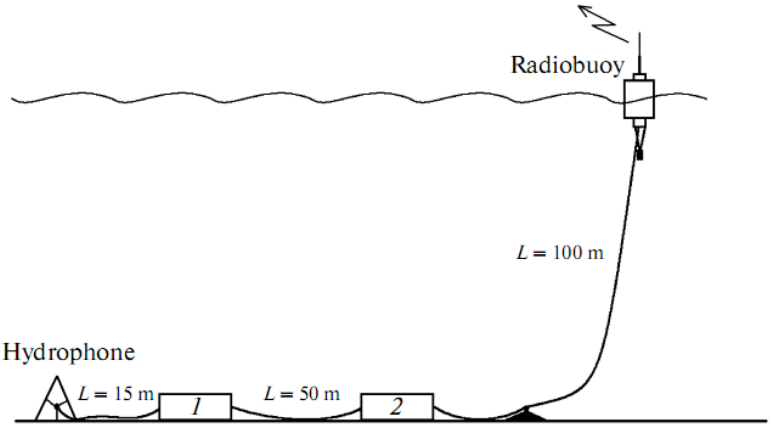

b)

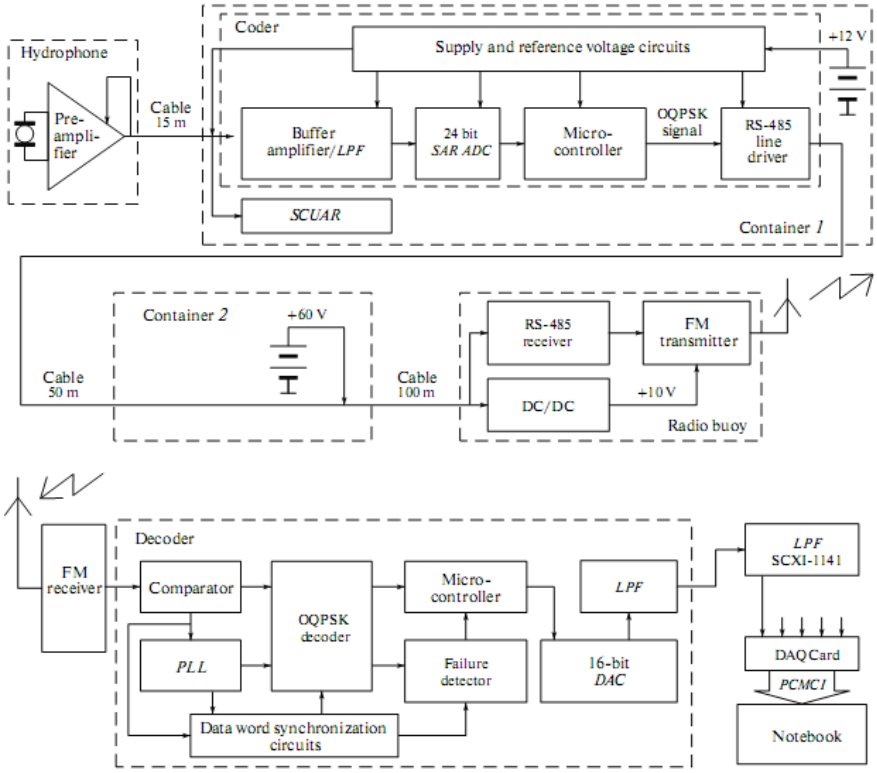

Fig. S1. (a) Schematic drawing of the telemetric acoustic station mooring and (b) block diagram of the electronics including the shore based receiving and recording equipment (from Kovzel & Rutenko 2009).

Supplement 2. Additional analysis post-survey of sound source verification data.

The safety range calculations performed at the start of the seismic survey relied on simplifications that enabled the timely assessment of safety radii based on the acoustic data alone, namely assuming that the strongest pulse arrival at the proximal receiver denoted the CPA and using the corresponding pulse measurements and nominal deployment setbacks for the three acoustic recorders to define the level-range pairs. These assumptions were made so as to lean toward a precautionary estimate. At a later date, having obtained GPS navigational data for the seismic survey vessel, a more accurate computation of the level-range regression formula that accounted for pulse strength variability was performed based on the measured levels for several pulses near CPA. Fig. S2 shows the measured rms pulse levels at the three sensors M1-M3 over a period of a few minutes after the start of the seismic line, as the source passes the CPA. The irregular strength of the pulses, most likely attributable to small operating variations between the two airgun arrays being fired in alternating sequence, is clearly observable in these traces.

The GPS positional information for the seismic vessel was compensated for the layback (distance behind the vessel) of the seismic source by offsetting the time base of the positional data so that the geographic CPA coincided with the well-defined culm of the sound level trace at the proximal sensor M1. This equating of layback to time delay is justifiable over an analysis period spanning only a few minutes, over which the speed of the seismic vessel can be considered to be constant. A subset of received pulse levels at the three sensors for a few consecutive pulses on either side of the CPA time, along with the corresponding computed distances between the seismic source and each of the sensors, was used as the basis for the level-range regression. The subset of levels was truncated at a roll-off of 3 dB from the CPA maximum on receiver M1 and replicated with the same temporal bounds for the other two sensors.

The inset table in Fig. S3 summarizes the pulse levels at the three sensors and the corresponding ranges; the figure shows the massed data plotted as a semi-log graph of level vs. range with the best-fit regression (solid straight line) and corresponding formula. An established practice to provide conservative safety range estimates in SSV studies is to add an offset to the best fit function (by adding an offset to the constant term) so that the line exceeds 90% of the measured data. This 90% excess line (dashed) and corresponding formula are also presented in the figure.

The best-fit regression formula yields the following distances for rms SPL threshold values of 180 and 190 dB re µPa:

r_180dB = 1205m r_190dB = 517m

These ranges are consistent with the safety radii obtained from the initial analysis. With the precautionary adjustment based on the 90% excess line the safety radius for 180 dB would be increased to 1322m.

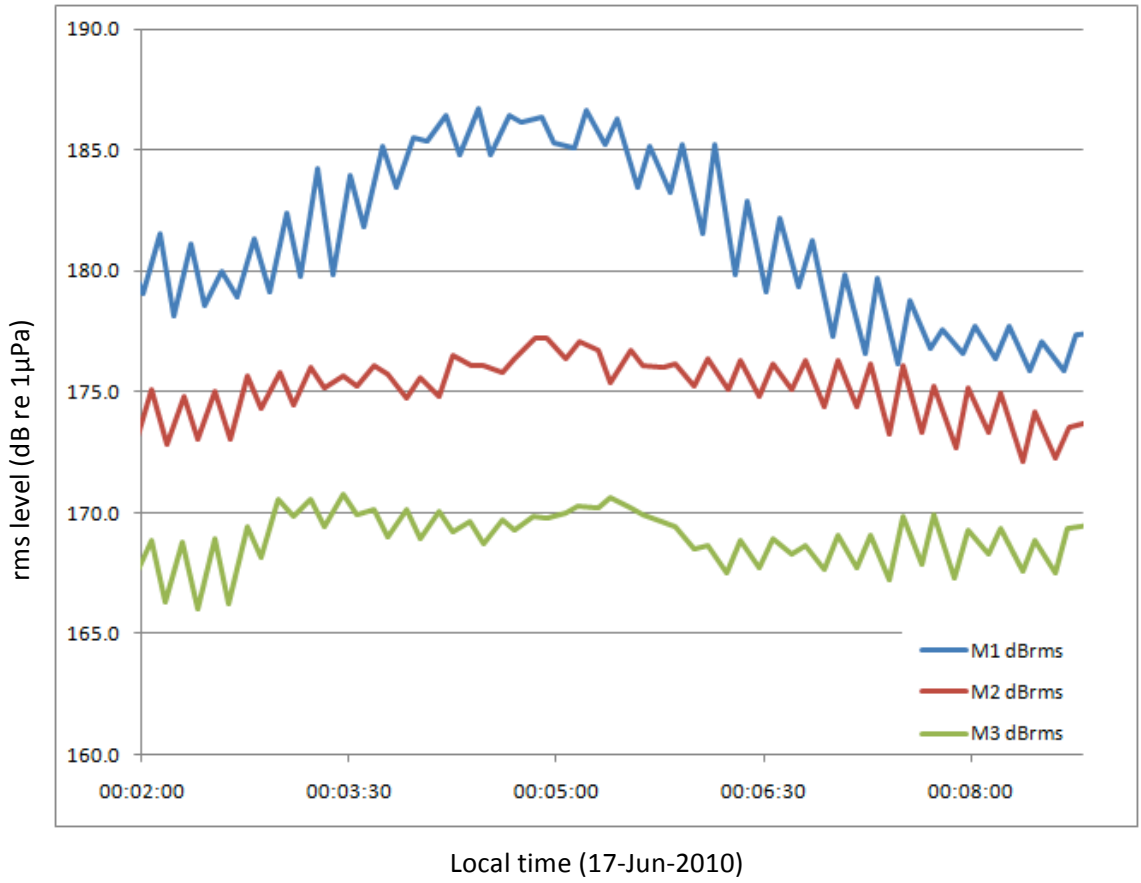

Fig. S2. Received rms levels at the three mini AUAR sensors over the period surrounding the CPA.

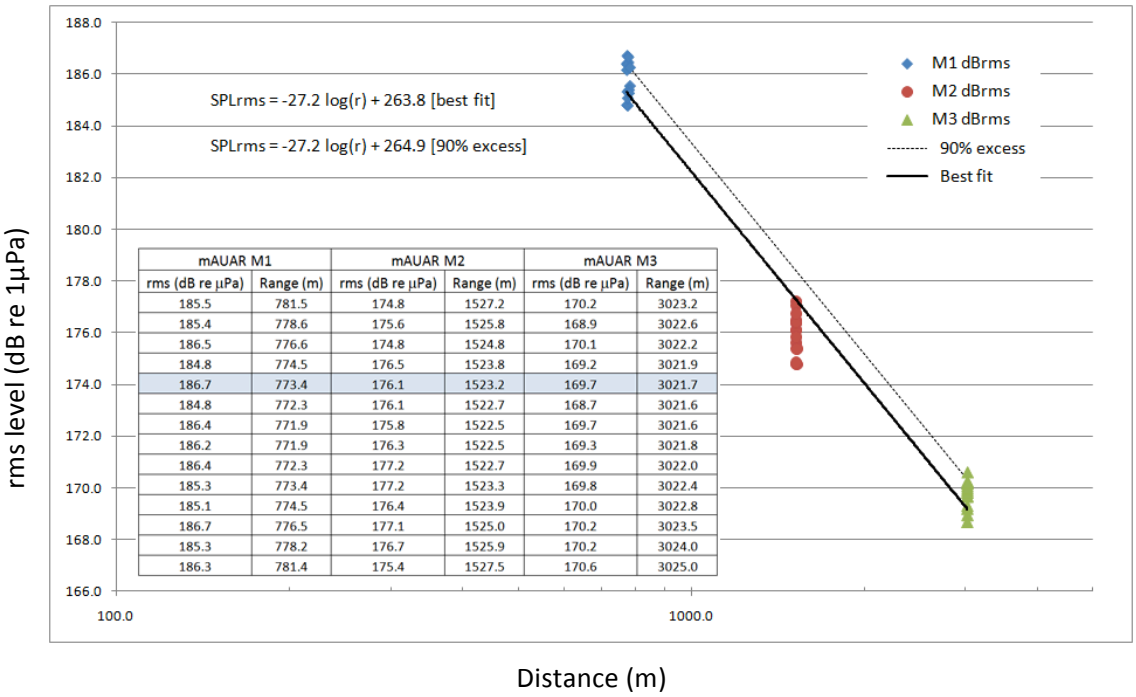

mAUAR M1		mAUAR M2		mAUAR M3	
rms (dB re µPa)	Range (m)	rms (dB re µPa)	Range (m)	rms (dB re µPa)	Range (m)
185.5	781.5	174.8	1527.2	170.2	3023.2
185.4	778.6	175.6	1525.8	168.9	3022.6
186.5	776.6	174.8	1524.8	170.1	3022.2
184.8	774.5	176.5	1523.8	169.2	3021.9
186.7	773.4	176.1	1523.2	169.7	3021.7
184.8	772.3	176.1	1522.7	168.7	3021.6
186.4	771.9	175.8	1522.5	169.7	3021.6
186.2	771.9	176.3	1522.5	169.3	3021.8
186.4	772.3	177.2	1522.7	169.9	3022.0
185.3	773.4	177.2	1523.3	169.8	3022.4
185.1	774.5	176.4	1523.9	170.0	3022.8
186.7	776.5	177.1	1525.0	170.2	3023.5
185.3	778.2	176.7	1525.9	170.2	3024.0
186.3	781.4	175.4	1527.5	170.6	3025.0

Fig. S3. Semi-log regression through rms levels vs. range from the source, along with 90% excess line. The inset table shows the data used in the regression (the triplet of levels that were used in the initial calculation of safety radii is highlighted for reference).